

Normal internal coordinates, force fields, and vibrational study of species derived from antiviral adamantidine

Silvia Antonia Brandán 

Cátedra de Química General, Instituto de Química Inorgánica, Facultad de Bioquímica, Química y Farmacia, Universidad Nacional de Tucumán, Tucumán, Argentina

Correspondence

Silvia Antonia Brandán, Cátedra de Química General, Instituto de Química Inorgánica, Facultad de Bioquímica, Química y Farmacia, Universidad Nacional de Tucumán, Ayacucho 471, (4000) San Miguel de Tucumán, Tucumán, Argentina.
Email: Silvia.brandan@fbqf.unt.edu.ar

Funding information

Consejo de Investigaciones, Universidad Nacional de Tucumán, Grant/Award Number: 26/D608

Abstract

Complete vibrational assignments have been performed for free base, cationic, and hydrochloride species derived from antiviral adamantidine by a combination of hybrid B3LYP with the 6-31G* and 6-311++G** basis sets and the scaled quantum force field methodology. Normal internal coordinates and scaling factors were used to obtain the harmonic force fields and scaled force constants of three species in gas phase and in aqueous solution. Bond lengths and angles of cationic and hydrochloride species show very good concordances with experimental adamantinium azide. The cationic species reveals a higher solvation energy value compared with antiviral agents; however, brincidofovir, the antiviral used for Ebola disease, presents a higher reactivity in contrast to adamantidine. A positive value of Mulliken charge on N1 of hydrochloride species in solution could justify the ionic character of the H29...Cl30 bond as it is possible to observe by bond order and atoms in molecules calculations. The hydrochloride species is the most reactive in both media, while the cationic species is the least reactive. High electrophilicity and nucleophilicity indices of cationic species in both media justify its higher hydration. Good concordances were observed between experimental and predicted ¹H and ¹³C NMR and electronic spectra. In solution, the three species are present as demonstrated by the experimental ultraviolet-visible spectrum of hydrochloride adamantidine.

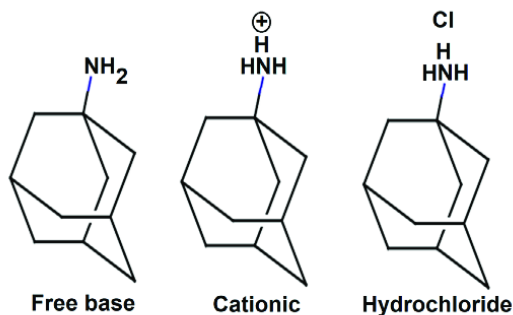
KEYWORDS

adamantidine, DFT calculations, force fields, structural properties, vibrational analysis

1 | INTRODUCTION

The study of adamantidine hydrochloride mass spectrum has revealed that the amino substituent is an ionic species, as in the crystalline structure of adamantinium azide.^[1,2] So far, the infrared and Raman spectra of adamantidine hydrochloride, free base, and cationic species of adamantidine are not assigned. These three structures of antiviral adamantidine are shown in Scheme 1. On the other hand, the combination of theoretical ab initio calculations with the vibrational spectra and the scaled quantum mechanical force field (SQMFF) methodology are very useful tools to assess reliable harmonic force fields and force constants, as suggested by Pulay et al.^[3] and as was reported for species with different fused rings.^[4-6]

The aims of this work are: (a) to optimize the free base, cationic, and hydrochloride species of adamantidine in gas phase and aqueous solution by using functional hybrid B3LYP with the 6-31G* and 6-311++G** basis sets^[7,8]; (b) to predict atomic charges, molecular electrostatic potentials (MEPs), stabilization energies, solvation energies, topological properties, and frontier orbitals in both media using the better basis set; and (c) to perform the complete vibrational assignments of three species of adamantidine by using the available infrared and Raman spectra and obtain the normal internal coordinates of each species by using the SQMFF methodology and the MOLVIB program.^[3,9,10] Then, the predicted properties for the three species of adamantidine are compared with those reported for antiviral agents.^[4,11-13] In addition, to verify the



SCHEME 1 Structures of free base, cationic, and hydrochloride species of amantadine

reproducibility of theoretically optimized structures of free base, cationic, and hydrochloride species, the predicted ^1H and ^{13}C NMR spectra were compared with the corresponding experimental ones available from the literature. The ultraviolet-visible spectra for the three species in aqueous solution were also predicted by using the same level of theory.

2 | MATERIAL AND METHODS

The *GaussView* program^[14] was used to model the free base, cationic, and hydrochloride structures of amantadine according to the crystalline structure of amantadinium azide,^[2] while its optimizations in the gas phase and aqueous solution were performed with the functional hybrid B3LYP and the 6-31G* and 6-311++G** basis sets by using the Revision A.02 of Gaussian program.^[7,8,15] The integral equation-formalism polarizable continuum model (IEF-PCM) and universal solvation methods^[16-18] were used to optimize the three structures in solution, while the MOL-DRAW program was used to calculate the volumes of all species at the same level of theory.^[19] The IEF-PCM calculation with radii and nonelectrostatic terms for Truhlar and coworkers' solvation model density (SMD) solvation model is recommended for computing the ΔG of solvation, which was accomplished by performing gas phase and SMD calculations and taking into consideration the differences between the resulting energies (E solution-E gas phase). Then, the energies due to the nonelectrostatic term (ΔG_{ne}) are included in total energy, and for this reason, this value must be subtracted from the total value. Hence, ΔG (kJ/mol) = E_{solution} (kJ/mol) - E_{gas} (kJ/mol) - ΔG_{ne} , where the latter term is obtained from calculations in solution by using the self-consistent reaction force (SCRF)=SMD option and the Gaussian 09 program.^[15-18] An example of these calculations can be seen from www.gaussian.com by using keywords Gaussian 09 and the SCRF option.

To investigate possible intramolecular interactions, atomic charges, MEPs, acceptor-donor energies, and topological properties were calculated with the natural bond orbital (NBO) and AIM 2000 programs.^[20-23] The differences between both frontier orbitals were also computed to calculate the gap values and the chemical potential (μ), electronegativity (χ), global hardness (η), global softness (S), global electrophilicity index (ω), and global nucleophilicity index (E) descriptors.^[11-13] On the other hand, the electronic spectra of three species in aqueous solution were predicted by using the time-dependent density functional theory (DFT) calculations (TD-DFT), while the gauge-including atomic orbital (GIAO) method was used to predict the ^1H and ^{13}C NMR chemical shifts in the same medium.^[24] Normal internal coordinates of three species of amantadine and transferable scaling factors were used in the determination of corresponding harmonic force fields by using the SQMFF methodology and the MOLVIB program.^[3,9,10] The normal internal coordinates related to the NH_2 group of free base was considered with C_{2v} symmetry, while the NH_3^+ groups of cationic and hydrochloride groups were considered with C_{3v} symmetries. In the assignments, only potential energy distribution (PED) contributions $\geq 10\%$ were used, while the Raman predicted in activities were corrected to intensities with recommendable equations.^[25,26]

3 | RESULTS AND DISCUSSION

3.1 | Optimizations in both media

Optimized theoretical structures of free base, cationic, and hydrochloride species of amantadine and labelling of atoms can be seen in Figure 1. The three-dimensional shape of the molecules can be seen in Figures S1-S3.

The properties calculated using both B3LYP/6-311++G** and B3LYP/6-31G* hybrid methods are presented in Table 1. Thus, total energy uncorrected and corrected by zero point vibrational energy (ZPVE) for the three amantadine species in both media are presented along with dipolar moment and volume values and their corresponding variations by using both methods. With both basis sets, the three species present high

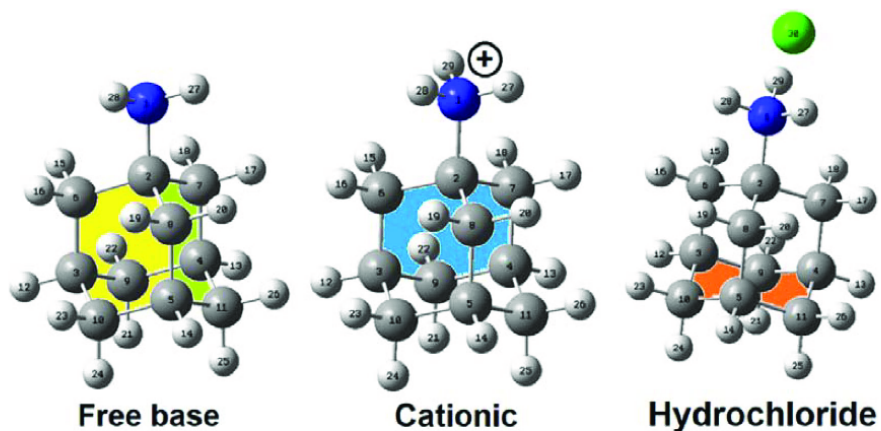


FIGURE 1 Structures of free base, cationic, and hydrochloride species of amantadine and atoms labelling. (yellow), R1 ring, C8-C2-C6-C3-C10-C5; (green), R2 ring, C8-C2-C7-C4-C11-C5; (blue), R3 ring, C7-C2-C6-C3-C9-C4; and (orange), R4 ring, C3-C9-C4-C11-C5-C10

TABLE 1 Calculated total energies (E), dipole moments (μ), and volumes (V) of three species of amantadine in gas and aqueous solution phases

B3LYP/6-311++G** Method					
Medium	E (Hartrees)	ZPVE	μ (D)	V (\AA^3)	ΔV (\AA^3)
Free base					
GAS	-446.1954	-445.9367	1.27	180.2	0.1
PCM	-446.2012	-445.9360	2.18	180.3	
Cationic					
GAS	-446.5709	-446.2971	7.86	182.4	-0.2
PCM	-446.6706	-446.2961	11.03	182.2	
Hydrochloride					
GAS	-907.0491	-906.7788	8.70	206.1	1.5
PCM	-907.0373	-906.7652	14.90	207.6	
B3LYP/6-31G* Method					
Medium	E (Hartrees)	ZPVE	μ (D)	V (\AA^3)	ΔV (\AA^3)
Free base					
GAS	-446.0723	-445.8113	1.24	180.1	-0.1
PCM	-446.0771	-445.8165	1.90	180.0	
Cationic					
GAS	-446.4542	-446.1782	8.06	182.9	-0.6
PCM	-446.5527	-446.2770	11.01	182.3	
Hydrochloride					
GAS	-906.8919	-906.6193	8.71	206.8	1.8
PCM	-906.9278	-906.6526	14.03	208.6	

dipole moment values in solution. The hydrochloride species shows high value, but the highest volume is observed for this species by using the B3LYP/6-31G* method. Both free base and hydrochloride species in the gas phase show practically the same dipole moment values, with both methods showing a change in solution. On the other hand, the volumes predicted for the cationic species with both basis sets present almost the same values. Only for the free base, the volume variations in both media are influenced by the size of basis set showing a slight contraction in volume with the 6-31G* basis set and an expansion in volume with the other one.

The high dipole moment values observed for the cationic and hydrochloride species in solution suggest the hydration of both species with water molecules. In addition to the magnitudes, different orientations of dipole moment vectors are observed in the three species in both media at the B3LYP/6-311++G** level of theory (Figure 2). Thus, in the free base, the vectors are located from the center moving towards the C5 atom, while in the cationic species, the vectors are located between the C2-N1 bonds, moving toward the outside. On the other hand, in the case of the hydrochloride species, the vectors originate closer to the C2 atoms, and they are directed toward the C5-H14 bonds. These different behaviors of vectors can have some influence on the properties of species, especially in aqueous solution. Hence, the solvation energies should be computed in order to see if the dipole moments have an effect on those parameters. Therefore, from the differences between the E values in aqueous solution and in gas phase, the corrected solvation energies (ΔG_c) were computed taking into account the total nonelectrostatic terms. Hence, $\Delta G_c = E_{\text{solution}} - E_{\text{gas}} - \Delta G_{\text{ne}}$. Thus, the ΔG_c values for free base, cationic, and hydrochloride species of amantadine by using the hybrid B3LYP/6-311++G** and B3LYP/6-31G* methods are summarized in Table 2.

These results show that the B3LYP/6-31G* method predicts low solvation energy values for the three species of amantadine, and the cationic species present high values because these species are charged in solution. For these reasons, these species with charges are most hydrated in aqueous solution. The free base of amantadine presents two donors (N–H) and one acceptor atom (N) H bonds, while the cationic and hydrochloride species have three donors and one acceptor atom H bonds. Hence, in these two latter species, higher hydrations are expected compared

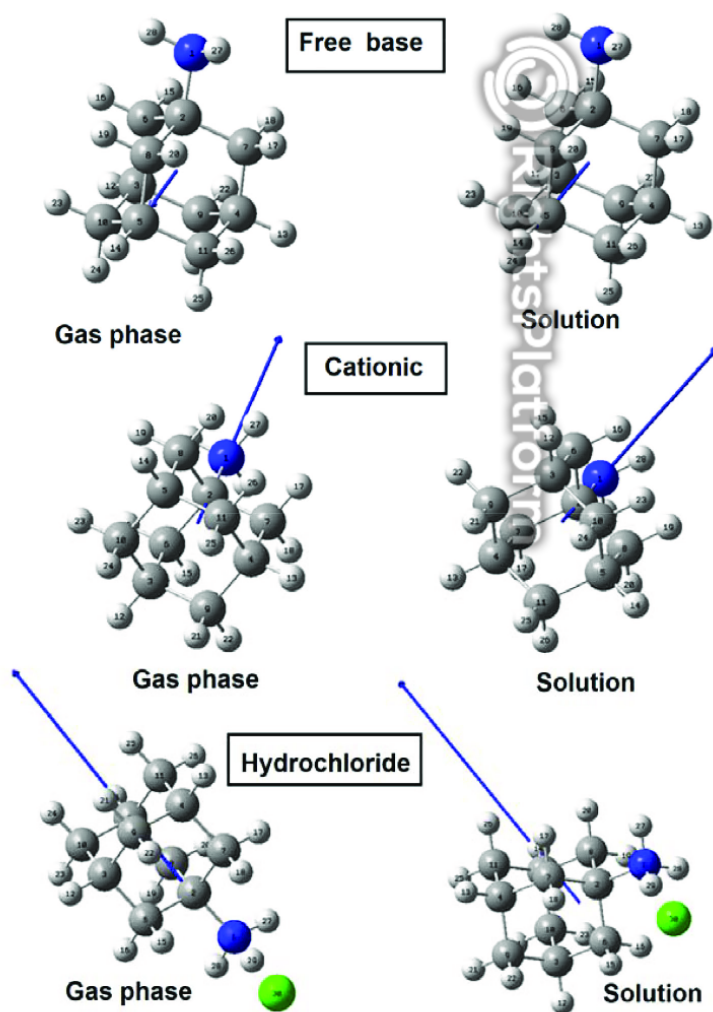


FIGURE 2 Orientations and directions of dipole moment vectors for the free base, cationic, and hydrochloride species of amantadine in both media by using the B3LYP/6-311++G** level of theory

TABLE 2 Corrected and uncorrected solvation energies by the total nonelectrostatic terms of three species of amantadine by using the hybrid B3LYP/6-311++G** and B3LYP/6-31G* methods

Amantadine ^a			
Solvation energy (kJ/mol)			
Condition	ΔG_{un}	ΔG_{ne}	ΔG_c
B3LYP/6-311++G** method			
Free base	-15.21	7.86	-23.07
Cationic	-261.51	14.84	-276.35
Hydrochloride	-100.19	14.84	-115.03
B3LYP/6-31G* method			
Free base	-12.59	7.73	-20.32
Cationic	-258.36	14.88	-273.24
Hydrochloride	-94.17	14.84	-109.01

Abbreviations: ΔG_{un} , uncorrected solvation energies; ΔG_{ne} , total nonelectrostatic terms; ΔG_c , corrected solvation energies.

^aThis work.

with the free base. These values for the three species of amantadine are compared with values predicted with the B3LYP/6-31G* method for antiviral agents, such as isothiazol (-37.51 kJ/mol), thymidine (-116.16 kJ/mol), cidofovir (-169.21 kJ/mol), and brincidofovir (-227.34 kJ/mol), with the value predicted for foscarnet using the B3LYP/6-311++G** method (-219.64 kJ/mol).^[4,11,12] The differences observed among all values of those species can be justified by the presence of acceptor and donor groups of H bonds. Thus, the free base presents lower values compared with isothiazole because this antiviral species has only one N-H bond, two N atoms, and the SH and C=N groups; hence, a higher hydration is expected for isothiazole in solution. The high value of cationic species could be justified by the positive charge and higher electrophilicity, while the hydrochloride species of amantadine has a slightly lower value than thymidine.

3.2 | Geometrical parameters in both media

A structural study is necessary to perform the vibrational analysis, and for this reason, the theoretical parameters calculated for the three species of amantadine should be compared with the corresponding experimental ones. Thus, in Table 3, the calculated bond lengths and angles and the dihedral angles for the three species of amantadine are presented in the two media using the B3LYP/6-311++G** level of theory. Here, the optimized geometrical parameters were compared with those corresponding to amantadinium azide^[2] and *N*-(2-hydroxybenzyl)adamantan-1-aminium chloride^[28] through the root-mean-square deviation (RMSD) values. As detailed in Table 3, it is possible to observe that the bond lengths and angles for the cationic and hydrochloride species show lower RMSD values as expected because those two compared compounds are present in the structures of NH₃ groups as two amantadine species.

In general, the structural parameters predicted for the three amantadine species correspond with those observed in other experimental structures.^[27-29] Besides, for both cationic and hydrochloride species, the RMSD values of bond lengths decrease in solution from 0.024 to 0.018 to 0.012 to 0.011 Å, while the free base species show RMSD values between 0.031 and 0.021 Å. If the bond angles are evaluated, a better correlation is observed for cationic and hydrochloride species, but low RMSD values (2.1°-0.2°) are observed when the predicted values are compared with the experimental parameters of amantadinium azide,^[2] which decrease in solution, compared with the values in gas phase. The free base presents RMSD values of bond angles between 2.6° and 1.7°, different from those predicted for cationic and hydrochloride species. A very important result is observed in all dihedral angles because, during the optimizations, the cationic and hydrochloride species change the signs in significant form, but the free base shows the lowest value in solution when they are compared with that corresponding to the amantadinium azide.^[2] This observation is justified because the free base is protonated in solution; hence, in this species, the NH₂ group is similar to the NH₃ one. In the hydrochloride species, the dihedral angles practically show the highest values because some angles change the signs with the optimization. In general, the dihedral angles present lower RMSD values when these are compared with those corresponding to amantadinium azide.^[2]

3.3 | Charges, MEP, and bond orders studies

Previous works on free base, cationic, and hydrochloride S(-) and R(+) species derived from scopolamine alkaloid and antihistaminic promethazine have evidenced that the behaviors of those three species in different media can be quickly explained by atomic charges, MEPs, and bond orders (BOs).^[5,6] Hence, three types of atomic charges were also analyzed in the three species of amantadine because, normally, these charges present

TABLE 3 Comparison of calculated geometrical parameters for the free base, cationic, and hydrochloride species of amantadine in gas phase and aqueous solution compared with the corresponding experimental ones for amantadinium azide^[27] and *N*-(2-Hydroxybenzyl)adamantan-1-aminium chloride

Parameters	B3LYP/6-31G** ^a						Exp ^b	Exp ^c
	Free base		Cationic		Hydrochloride			
	Gas	PCM	Gas	PCM	Gas	PCM		
Bond lengths (Å)								
N1-C2	1.469	1.477	1.548	1.515	1.500	1.511	1.504	1.517
C2-C6	1.542	1.540	1.534	1.534	1.540	1.536	1.523	1.534
C2-C7	1.542	1.540	1.533	1.534	1.540	1.536	1.522	1.534
C2-C8	1.550	1.546	1.533	1.535	1.539	1.536	1.525	1.514
RMSD ^b	0.031	0.026	0.018	0.011	0.016	0.011		
RMSD ^c	0.026	0.021	0.024	0.011	0.014	0.012		
Bond angles (°)								
N1-C2-C6	108.6	109.1	108.0	108.5	108.4	108.8	108.5	109.0
N1-C2-C7	108.6	109.1	108.0	108.5	108.3	108.8	109.1	111.0
N1-C2-C8	113.6	112.4	108.0	108.6	110.6	108.7	109.1	108.1
C6-C2-C7	108.6	108.8	110.8	110.3	109.7	110.2	110.1	108.4
C6-C2-C8	108.5	108.5	110.8	110.3	109.7	110.0	109.9	109.7
C8-C2-C7	108.5	108.5	110.8	110.3	109.7	110.0	109.9	110.3
RMSD ^b	2.1	1.7	0.9	0.4	0.7	0.2		
RMSD ^c	2.6	2.1	1.7	1.3	1.6	1.2		
Dihedral angles (°)								
N1-C2-C8-C5	179.9	-180.0	179.9	179.9	-179.9	-180.0	-179.7	-177.6
N1-C2-C6-C3	177.2	178.2	-179.9	179.9	178.7	-179.9	179.5	178.5
N1-C2-C7-C4	-177.2	-178.2	179.9	-179.8	-178.7	179.9	-179.6	178.0
RMSD ^b	207.6	1.1	359.5	207.6	>1000	179.9		
RMSD ^c	291.0	205.7	292.3	292.0	>>1000	>>1000		

Note: RMSD values in letter bold.

^aThis work.

^bWang et al.^[27] for amantadinium azide.

^cRong^[28] for *N*-(2-Hydroxybenzyl)adamantan-1-aminium chloride.

different values among them and in both media. Hence, atomic Merz-Singh-Kollman (MK), Mulliken, and NPA charges, together with MEPs and BOs, expressed as Wiberg indices, have been calculated for those three species of amantadine in both media using the B3LYP/6-311++G** level of theory. These parameters are presented only for the N1, C2, C6, and C8 atoms in Table 4 because these atoms structurally belong to the C-NH₂ group in the free base and to the C-NH₃ groups corresponding to cationic and hydrochloride species (See Figure 1). In Figure 3, the behaviors of those three charges are given on the N1, C2, C6, and C8 atoms of three species of amantadine in both media.

The exhaustive analyses of figures show that the MK (blue lines) and NPA (green lines) charges present similar behaviors in both media but different from Mulliken charges (red lines). The three charges on C2 atoms of three species in both media present positive values, where high values are observed in the MK charges. On the contrary, the Mulliken charges on all C2 atoms show negative values, but higher values are seen on those atoms of cationic and hydrochloride species. Note that the Mulliken charge on the N1 atom of hydrochloride species in solution shows a positive value, while the other charges show negative values on these atoms in the two media. This observation could probably be justified by the transformation of the covalent H29-C130 bond in gas phase between both atoms to ionic N1-H29... Cl30 bond in solution, as evidenced by AIM calculations. On the other hand, a very important result is that the three charges studied on the C6 atoms of cationic and hydrochloride species show practically the same values, and only few differences in the charges corresponding to the free base species in both media are observed.

The MEPs for the three species of amantadine in both media have been calculated using the Merz-Singh-Kollman scheme and the same level of theory, which can be seen in Table 4. For the atoms of the free base, the same values are observed in the two media, while slight differences can be seen on the atoms corresponding to the cationic and hydrochloride species. The distributions of charges in the three species are quickly observed by the different colorations shown on the mapped surfaces generated with the *GaussView* program.^[14] These red, blue, and green

TABLE 4 Mulliken, Merz-Kollman, and NPA charges (a.u.); molecular electrostatic potentials (MEP) (a.u.); and bond orders, expressed as Wiberg indices for the three species of amantadine in gas phase and in aqueous solution by using B3LYP/6-311++G** calculations

Gas						PCM				
Atoms	MK	Mulliken	NPA	MEP	BO	MK	Mulliken	NPA	MEP	BO
Free base										
1 N	-1.067	-0.230	-0.84655	-18.425	2.826	-1.053	-0.225	-0.838	-18.425	2.826
2 C	0.871	-0.279	0.11724	-14.743	3.991	0.879	-0.288	0.118	-14.743	3.992
6 C	-0.490	-0.532	-0.38425	-14.788	3.940	-0.499	-0.539	-0.385	-14.788	3.940
8 C	-0.594	-0.516	-0.39244	-14.787	3.945	-0.575	-0.510	-0.393	-14.786	3.946
Cationic										
1 N	-0.823	-0.034	-0.681	-18.101	3.307	-0.792	-0.021	-0.674	-18.097	3.311
2 C	0.673	-0.896	0.159	-14.542	3.919	0.710	-0.961	0.150	-14.545	3.921
6 C	-0.486	-0.365	-0.411	-14.619	3.926	-0.496	-0.341	-0.407	-14.620	3.927
8 C	-0.466	-0.365	-0.412	-14.619	3.926	-0.532	-0.346	-0.407	-14.620	3.927
Hydrochloride										
1 N	-0.459	-0.089	-0.759	-18.317	3.184	-0.436	0.363	-0.730	-18.272	3.243
2 C	0.795	-0.499	0.143	-14.695	3.958	0.774	-0.884	0.147	-14.674	3.949
6 C	-0.419	-0.432	-0.403	-14.760	3.923	-0.371	-0.437	-0.406	-14.744	3.922
8 C	-0.554	-0.500	-0.396	-14.749	3.939	-0.572	-0.345	-0.399	-14.732	3.936

colorations on the mapped MEP surfaces of three species indicate different regions of reactivity, as given in Figure 4. Thus, the free base and hydrochloride species show the three colors in different regions, different from the cationic one. The free base shows a strong red color on the lone pairs of N1 atom and light blue colors on the H27 and H28 atoms corresponding to NH₂ group, while in the hydrochloride species, the strong red color is observed on the C30 atom and the strong blue colors on the three H atoms of NH₃ group. On the other hand, the cationic species show blue colors on the entire surface because it is a positively charged species with a high MEP value (-0.20 a.u.). Then, the red color indicates nucleophilic sites, the blue color electrophilic sites, while the green regions are inert sites. In these sites, the reactions with potential biological electrophiles or nucleophiles occur. Hence, different reaction sites are evidenced in the three species of amantadine.

These mapped surfaces observed on the free base, cationic, and hydrochloride species of amantadine are similar to those S(-) and R(+) species of scopolamine alkaloid and antihistaminic promethazine.^[5,6]

The BO totals by atom, expressed as Wiberg indices, have been computed for the three species of amantadine with the NBO program by using the 6-311++G** level of theory.^[21] These results for the three species are presented in Table 4. The BOs for the free base present approximately the same values in both media, while few differences are observed for the cationic and hydrochloride species. However, the Wiberg bond index matrix in the natural atomic orbital (NAO) basis for the H29-Cl30 bond shows, for the hydrochloride species, a covalent character in gas phase (0.355), which is transformed to ionic in solution (N1-H29...Cl30) with a value of 0.123.

3.4 | NBO and AIM studies

The studies of stabilities in the three species of amantadine are interesting due to the presence of donor (N-H bonds) and acceptor H bonds (N atoms) corresponding to the NH₂ and NH₃ groups of their structures. These acceptor and donor groups have importance in pharmacological drugs, as in this case.^[30,31] Hence, the intramolecular interactions can be studied by using the second-order perturbation theory analyses of Fock matrix in the NBO Basis by using the NBO program and by using the AIM 2000 program.^[21-23] First, the studies of donor-acceptor interactions of three species of amantadine in both media by using the NBO program with the B3LYP/6-311++G** method reveal that the free base in both media present the only LP(1)N1 → σ*C2-C8 interaction with a value of 36.66 kJ/mol in gas phase, which decreases to 32.90 kJ/mol in solution. The cationic species does not show interactions in both media, but in the gas phase, the hydrochloride species shows the two LP(1)Cl30 → σ*N1-H29 and LP(4)Cl30 → σ*N1-H29 interactions with values of 43.22 and 559.16 kJ/mol, respectively. In solution, the latter LP(4)Cl30 → σ*N1-H29 interaction decreases to 125.65 kJ/mol. A higher energy value observed for the hydrochloride species in gas phase (602.38 kJ/mol) indicates that this species is more stable in both media than the other ones, but its stability decreases in solution. On the contrary, the cationic species probably does not present interactions because this species is hydrated, as supported by high solubility in the water of hydrochloride species and its higher solvation energy.

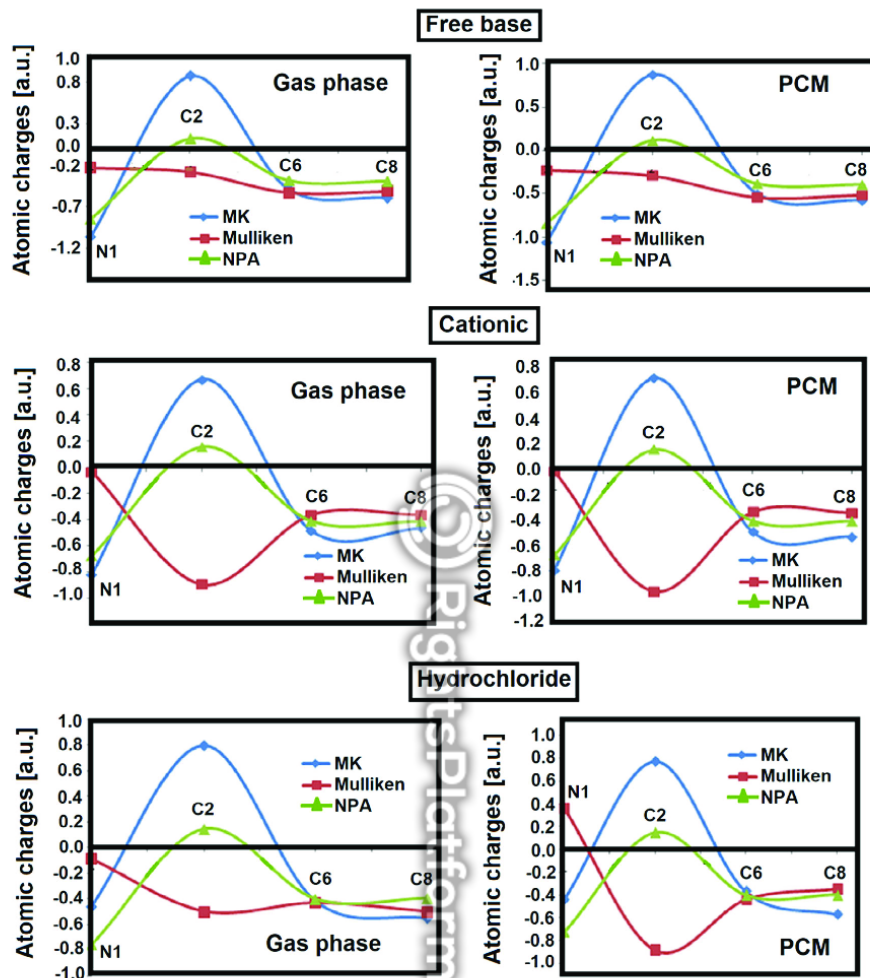


FIGURE 3 Calculated MK, Mulliken, and NPA charges on the N1, C2, C6, and C8 atoms corresponding to the free base, cationic, and hydrochloride species of amantadine in both media by using the B3LYP/6-311++G** method

Bader's theory of atoms in molecules is useful to investigate the characteristics or nature of the different types of interactions, such as intramolecular, H bonds, ionic, covalent polar, etc., with the topological properties by using the AIM 2000 program.^[22,23] Then, in the bond critical points (BCPs) and ring critical points (RCPs) for the three species in both media, the electron density, $\rho(r)$; the Laplacian values, $\nabla^2\rho(r)$; the eigenvalues ($\lambda_1, \lambda_2, \lambda_3$) of the Hessian matrix; and the $|\lambda_1/\lambda_3|$ ratio using the B3LYP/6-311++G** method have been calculated. The results have evidenced that, only for the hydrochloride species, new H bonds are formed in both media (BCPs), while for the three species, cage critical points (CCPs) are observed. These points are formed when several rings form a cage, and for these reasons, the topological properties for RCPs are not presented here. The topological properties predicted for CCPs and BCPs of free base, cationic, and hydrochloride species by using the B3LYP/6-311++G** method are presented in Table 5.

The ionic or highly polar covalent interactions (BCPs) show $\lambda_1/\lambda_3 < 1$ and $\nabla^2\rho(r) > 0$ (closed-shell interaction), while the eigenvalues of the Hessian matrix in the CCPs all have positive signs in the three species and approximately the same values in the two media. Molecular graphics of three species in gas phase can be observed in Figure 5, showing the H bond interaction (BCPs) of hydrochloride species in red color and the CCPs of three species in green colors. The only BCPs predicted for the hydrochloride species suggest a high stability for this species in both media. Note that the long distance observed for that species in solution suggests that the covalent bond in solution is transformed to ionic, supported by BO

FIGURE 4 Calculated electrostatic potential surfaces on the molecular surfaces of the free base, cationic, and hydrochloride species of amantadine in gas phase. B3LYP functional and 6-311++G** basis set. Isodensity value of 0.005

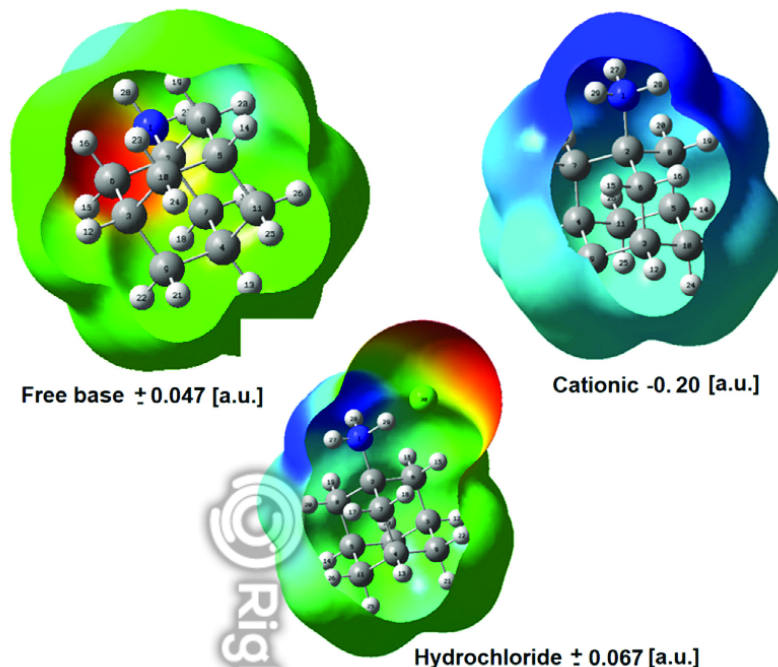


TABLE 5 Analysis of the bond critical points (BCPs) and ring critical points (RCPs) for the free base and cationic species of amantadine in gas phase and aqueous solution using the B3LYP/6-31G* method

B3LYP/6-311++G** Method								
Parameter ^a	Cage critical point						BCP	
	Free base		Cationic		Hydrochloride		H29...Cl30	H29...Cl30
	Gas	PCM	Gas	PCM	Gas	PCM	Gas	PCM
$\rho(r)$	0.0118	0.0119	0.0123	0.0123	0.0121	0.0122	0.0952	0.0340
$\nabla^2\rho(r)$	0.0724	0.0728	0.0741	0.0741	0.0734	0.0740	0.0148	0.0558
λ_1	0.0236	0.0237	0.0245	0.0246	0.0242	0.0244	-0.1734	-0.0420
λ_2	0.0242	0.0244	0.0246	0.0246	0.0244	0.0245	-0.1733	-0.0419
λ_3	0.0244	0.0246	0.0248	0.0248	0.0246	0.0248	0.3320	0.1398
$ \lambda_1 /\lambda_3$	0.9672	0.9634	0.9879	0.9919	0.9837	0.9839	0.5223	0.3004
Distances							1.664	2.118

^aParameters in a.u., distances in Å.

studies. Besides, if the hydrochloride species is ionic, as is usually expected because it is a salt, in solution, it is a cationic one, as was also observed in the three S(-) and R(+) species of scopolamine alkaloid and antihistaminic promethazine agent.^[5,6]

3.5 | Frontier orbitals and global descriptors studies

The gap values calculated from the frontier orbitals, highest occupied molecular orbital (HOMO), and lowest unoccupied molecular orbital (LUMO) are necessary parameters to predict reactivities, as recommended by Parr and Pearson,^[32] while the behaviors in the different media can be predicted using classical descriptors.^[4-6,11-13] In this study, the HOMO, LUMO, energy band gaps and the chemical potential (μ),

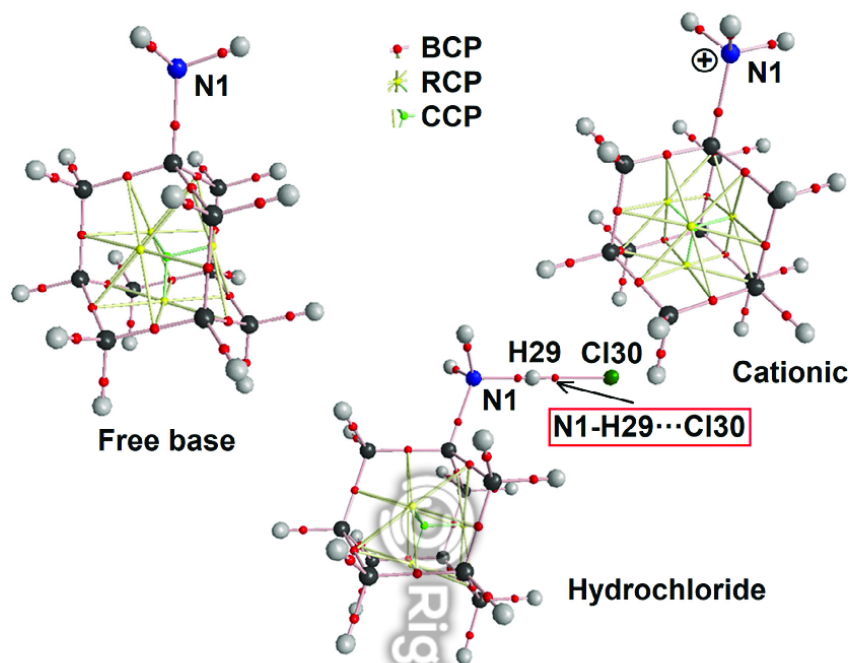


FIGURE 5 Molecular graphics of three species of amantadine in gas phase showing their H bond interactions by using the B3LYP/6-311++G** method

TABLE 6 Frontier molecular orbitals, HOMO and LUMO, gap values, and descriptors for the three amantadine species in gas phase and aqueous solution by using the B3LYP/6-311++G** level of theory

B3LYP/6-311++G** Method ^a						
Orbital	Free base		Cationic		Hydrochloride	
	Gas	PCM	Gas	PCM	Gas	PCM
HOMO	-6.4736	-6.5552	-11.6029	-11.5730	-6.3294	-6.4736
LUMO	-0.4218	-0.4299	-4.9253	-4.9606	-0.9334	-0.4218
GAP	6.0518	6.1253	6.6776	6.6124	5.3960	4.1116
Descriptors						
χ	-3.0259	-3.0627	-3.3388	-3.3062	-2.6980	-2.0558
μ	-3.4477	-3.4926	-8.2641	-8.2668	-3.6314	-3.3130
η	3.0259	3.0627	3.3388	3.3062	2.6980	2.0558
S	0.1652	0.1633	0.1498	0.1512	0.1853	0.2432
ω	1.9641	1.9914	10.2275	10.3351	2.4439	2.6695
E	-10.4324	-10.6965	-27.5922	-27.3317	-9.7975	-6.8109

$$\chi = -[E(\text{LUMO}) - E(\text{HOMO})]/2; \mu = [E(\text{LUMO}) + E(\text{HOMO})]/2; \eta = [E(\text{LUMO}) - E(\text{HOMO})]/2; S = 1/2\eta; \omega = \mu^2/2\eta; E = \mu \times \eta.$$

^aThis work.

electronegativity (χ), global hardness (η), global softness (S), global electrophilicity index (ω), and global nucleophilicity index (E) descriptors^[11–13] for the three species of amantadine in both media using the B3LYP/6-311++G** method are summarized in Table 6, along with the equations used to calculate the descriptors. In Table 7, these parameters reported for other antiviral agents are presented.^[4,11–13]